Using Modal Analysis and ODS Correlation to Identify Mechanical Faults in Rotating Machinery

Brian Schwarz, Shawn Richardson, Patrick McHargue, Mark Richardson
Vibrant Technology, Inc., Centennial, CO

Click here for the IMAC Power Point presentation.

ABSTRACT

Most power plants, oil refineries, and manufacturing plants worldwide have implemented machinery health monitoring programs for assessing the health of their rotating machinery and equipment. Digital vibration signals are the primary data used to detect and diagnose mechanical faults in operating machinery.

A common machine fault is called ***"soft foot"***. Soft foot is a lowering of the stiffness between a machine and its foundation.

In this paper, a modal model of a rotating machine on springs and several digital signal processing methods are used to create **first-order ODS's** for several mounting stiffnesses and internal force levels. Then, these **order-based ODS's** are used by a unique database search method called **FaCTs™**, to estimate the mounting stiffnesses and internal force levels in a rotating machine from **TWFs** derived from cellphone videos.

FaCTs™ correlates a ***currently acquired*** **ODS** with **ODS's** of known machine faults stored in a database. **FaCTs™** can be used to identify the location and amount of any mechanical fault based on its ***unique*** **ODS**. And **FaCTs™** becomes more accurate as ***more*** **ODS** ***data is acquired, labeled, and archived*** in a machine-based database. A typical **FaCTs™** bar chart is shown in Figure 1.

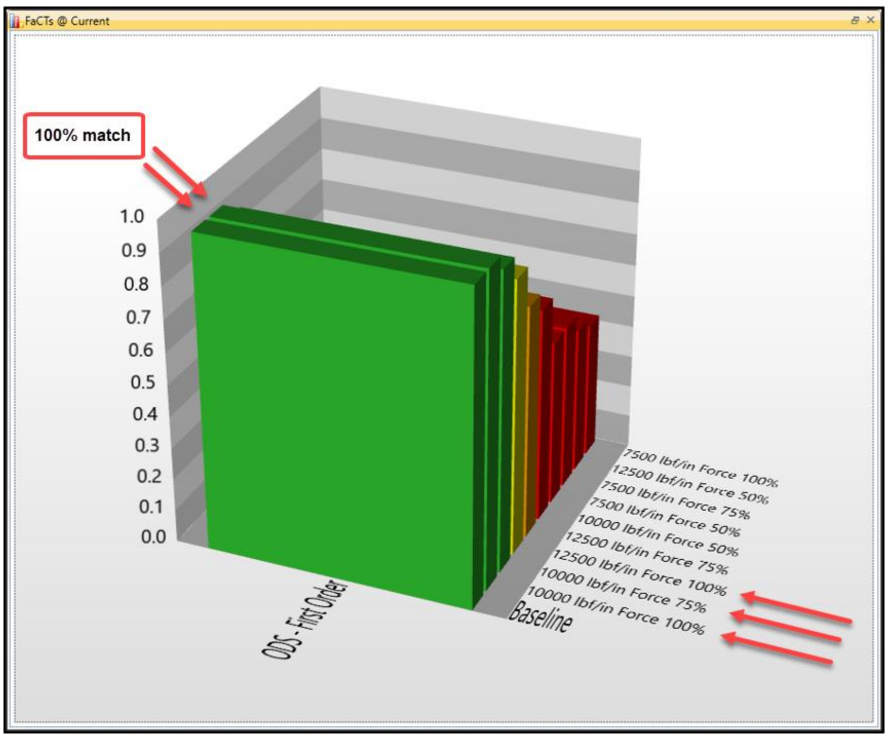

Figure 1. FaCTs™ Bar Chart

KEY WORDS

Time Waveform (**TWF**), Digital Fourier Transform (**DFT**), Operating Deflection Shape (**ODS**), Degree of Freedom (**DOF**), Neural Network (**NN**), Fault Correlation Tools (**FaCTs™**), Shape Difference Indicator (**SDI**)**,** Finite Element Analysis (**FEA**), Auto Power Spectrum (**APS**), Cross Power Spectrum (**XPS**), **ODS-FRF** (**APS** and **Phase** of an **XPS** relative to a reference), Structural Dynamics Modification (**SDM**), Multi-Input Multi-Output (**MIMO**) matrix model.

INTRODUCTION

Artificial Intelligence (**AI**) has recently become popular for interpreting the meaning of a set of data using a trained neural network. A trained **NN** models the human brain, which also must be trained with input data from the moment we are born and throughout our life.

Machine learning using an **NN** mimics the learning of a human brain. To train an **NN** to identify a machine fault, it must be given lots of data sets, each data set uniquely correlated with a mechanical fault and labeled as such. Then when given newly-acquired machine data as input, a trained **NN inference engine** will identify any mechanical fault if it was trained with similar data.

FaCTs™

At Vibrant Technology, we have developed an algorithm, called **FaCTs™**, which functions like a trained **NN**, but doesn't require training with lots of data. Given an experimentally derived **ODS**, **FaCTs** searches a database of ***labeled*** **ODS's**, each **ODS** labeled with a particular machine fault. Then a **FaCTs** bar chart of the ***ten closest matching*** **ODS's** is displayed together with the mechanical fault associated with each labeled **ODS**.

FaCTs™ uses a correlation coefficient between two shapes called the **Shape Difference Indicator (SDI)** [11], to search a database of archived and labeled **ODS's**. By comparing the **SDI** value of a current **ODS** with each archived **ODS** in the database, the ***ten highest*** **SDI** ***values*** and their ODS labels are displayed in a **FaCTs** bar chart. An example bar chart was shown in Figure 1.

- **FaCTs** has values between **0.0 & 1.0**
- **FaCTs** = **1.0** ➔ two **ODS's** are ***identical***
- **FaCTs above 0.9** ➔ two **ODS's** are ***similar***
- **FaCTs below 0.9** ➔ two **ODS's** are ***different***

In previous papers [3], [8] we presented a new method for extracting **TWFs** from frames of a video. This method together with traditional digital signal processing methods, has been used to further extract **order-based ODS's** [4]-[6] of an operating machine from a video. Using **ODS's** in animation, the machine's deformation can be visualized using frames of the video at ***slower speeds with higher amplitudes***.

ROTATING MACHINE

In a companion paper [10], **FaCTs™** was used to uniquely identify ***nine different unbalance cases*** of the rotating machine shown in Figure 2 using order-based **ODS's** extracted from cellphone videos. This machine has a variable speed motor connected to the rotor with a rubber belt. The motor speed was adjusted so that the rotor speed was ***approximately*** **1000 RPM** throughout all the cellphone video recordings. Those videos are also used in this paper.

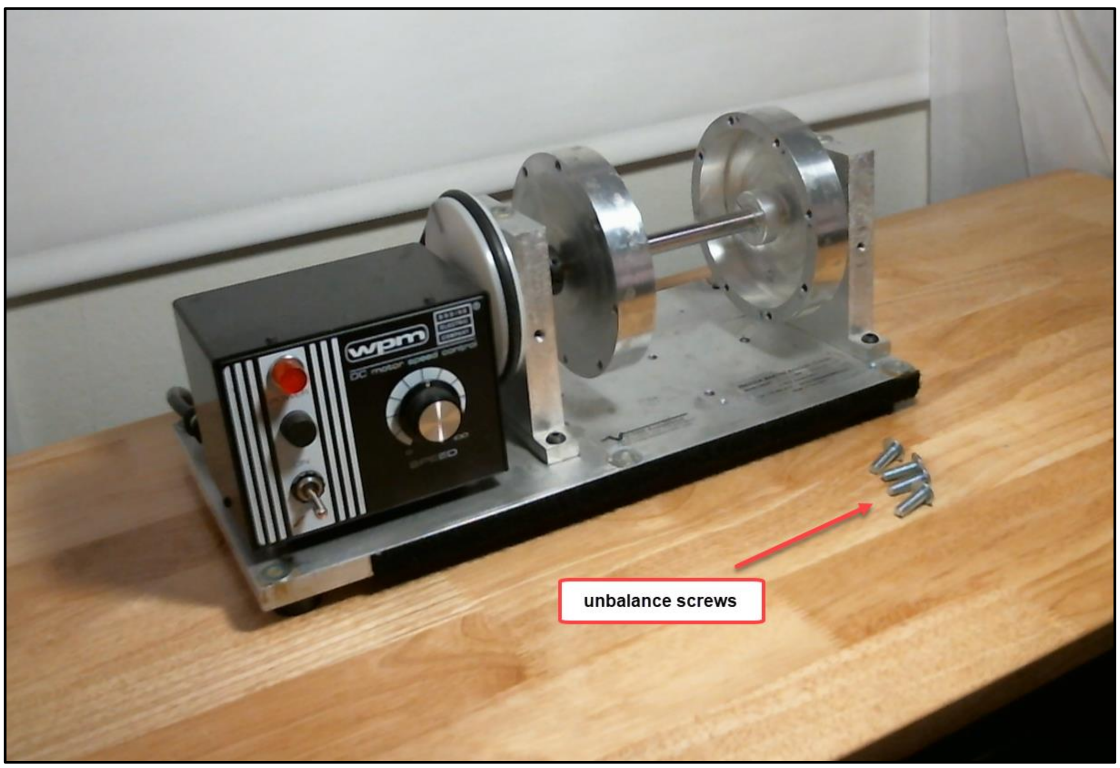

Figure 2. Rotating Machine Showing Unbalance Screws Added to Its Rotors

FEA Free-Body Modal Model

An **FEA model** with **free-free boundary conditions** was created for the **baseplate and bearing blocks** of the rotating machine. The FEA model was then solved for its ***first ten modes of vibration***. The deflection of an FEA bending mode shape is shown in Figure 3, together with the modal ***frequencies of the first ten modes*** of the machine.

Because the machine was modeled as a free body in space, its first six modes have zero frequency & damping, and have ***rigid-body mode shapes***. Three mode shapes are ***rigid body deflections in three translational directions*** and three mode shapes are ***three rotational deflections about three rotational axes***.

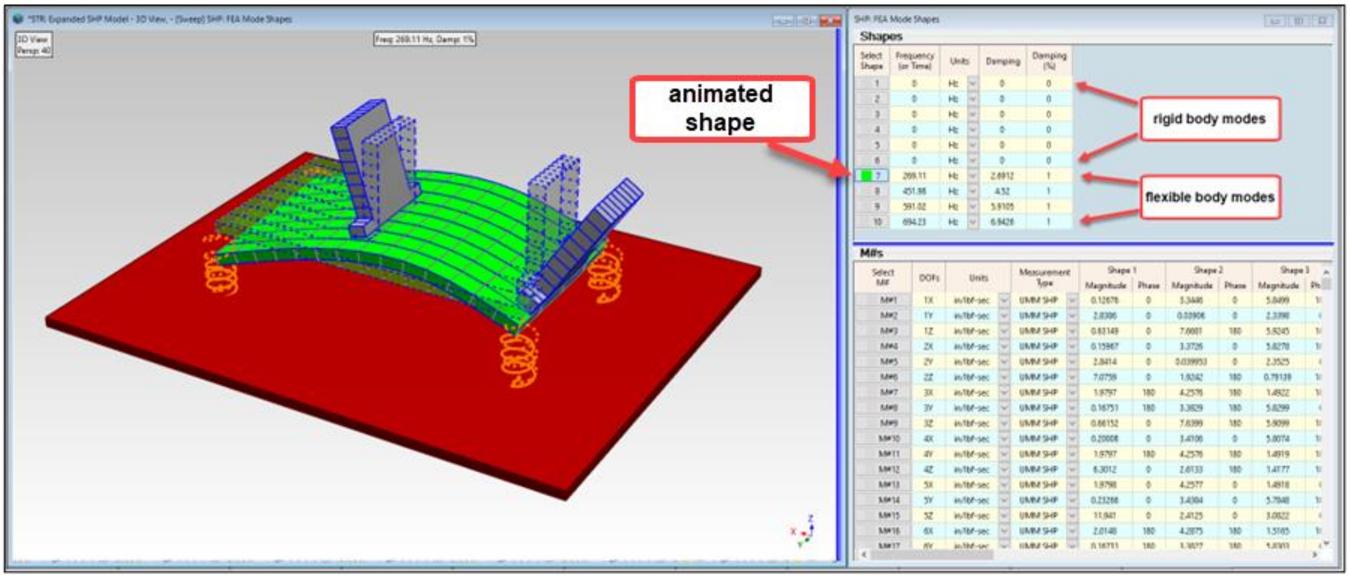

Figure 3. Bending Mode Shape of the Base Plate and Bearing Blocks

STRUCTURAL DYNAMICS MODIFICATION (SDM)

SDM [12] is a modeling algorithm also referred to as ***"eigenvalue modification"***. **SDM** calculates ***the new mode shapes*** of a mechanical structure caused by ***physical modifications*** to the structure. Modifications are modeled with industry-standard finite elements. The inputs and outputs of **SDM** are depicted in the diagram in Figure 4.

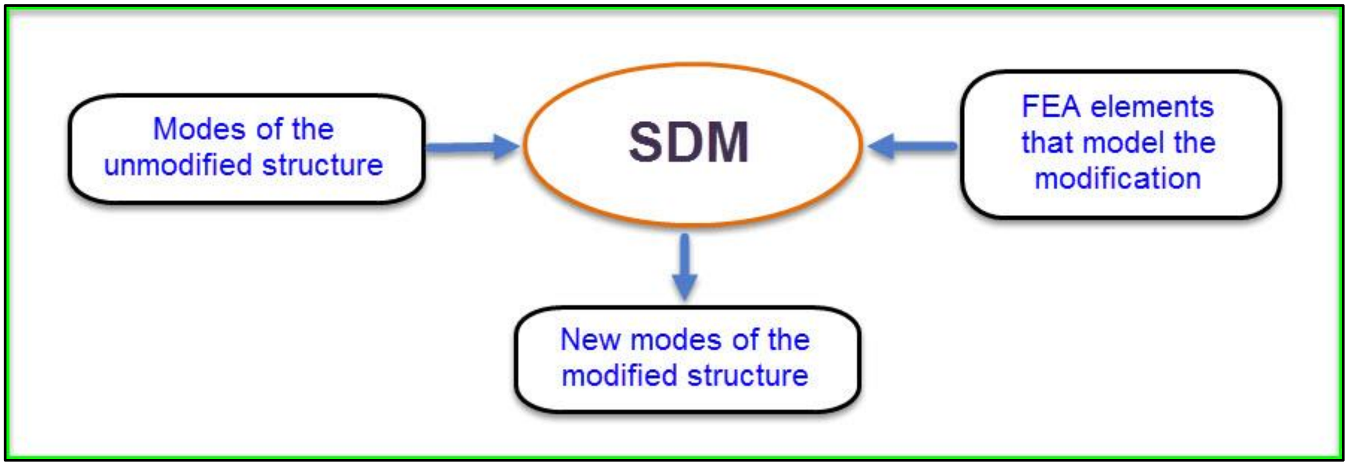

Figure 4. Structural Dynamics Modification (SDM)

In this paper, the mounting stiffnesses of the rotating machine resting on a ***"fixed"*** tabletop are modeled with four **FEA spring elements,** each one attached between a corner of the base plate and the ***"fixed"*** tabletop. The four springs between the base plate and the tabletop are also shown in Figure 3.

To model the machine attached to its fixed base with different mounting stiffness, the four **FEA** springs, (one between each corner of the base plate and the ***"fixed"*** tabletop), with modeled using ***five different mounting stiffnesses*** as inputs to **SDM**. **SDM** is then used to calculate the new modes of the machine for each stiffness case.

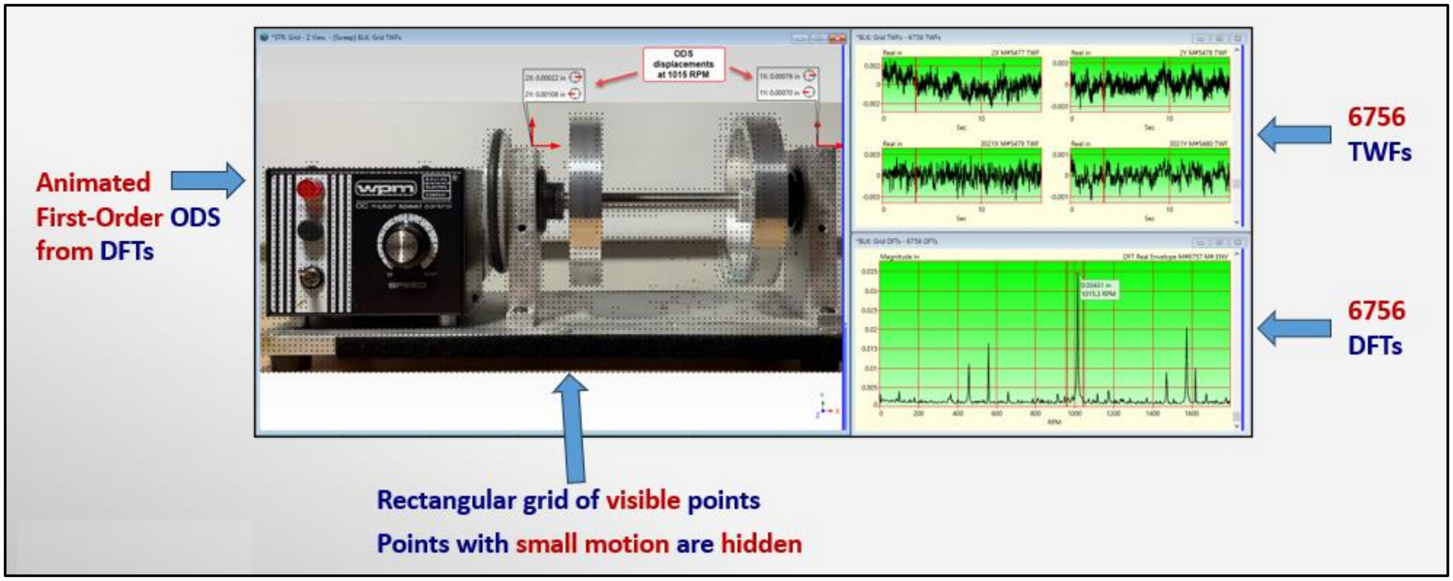

Figure 5. First-Order ODS Animated from DFTs

ODS-FRFs

Using **MEscope Video ODS™**, ***thousands of*** **TWFs** are typically extracted from a video recording of an operating machine. A unique frequency domain function called an **ODS-FRF** can be calculated from each response **TWF**. Not only can **ODS-FRFs** yield the **order-based ODS's** of rotating equipment with more accuracy, but they can be differentiated ***from displacement to velocity units*** which are commonly used to assess vibration levels in rotating equipment.

The ***magnitude*** of an **ODS-FRF** is the **APS** of a ***roving response*** **DOF** of a machine. The ***phase*** is the ***phase of the*** **XPS** between the response **DOF** and a ***fixed reference*** **DOF**.

An **ODS-FRF** carries the same engineering units as the response **TWF** from which was calculated. A **TWF** extracted from a video has ***units of displacement***. But because it is a frequency domain function, an **ODS-FRF,** (and a **DFT**), can be uniquely ***differentiated to velocity*** or acceleration units. But **TWF** windowing and spectrum averaging can be used to reduce extraneous noise from an **ODS-FRF**.

MIMO (MULTI-INPUT MULTI-OUTPUT) MATRIX MODEL

All modal analysis of the Input-Output dynamics of a mechanical structure is based on the **MIMO Matrix Model** shown in Figure 6.

Using the **MIMO Matrix Model**, **Output TWFs** can be calculated from **FRFs** & **Input TWFs**, **Input TWFs** can be calculated from **FRFs** & **Output TWFs**, and **FRFs** can be calculated from **Input TWFs** & **Output TWFs**.

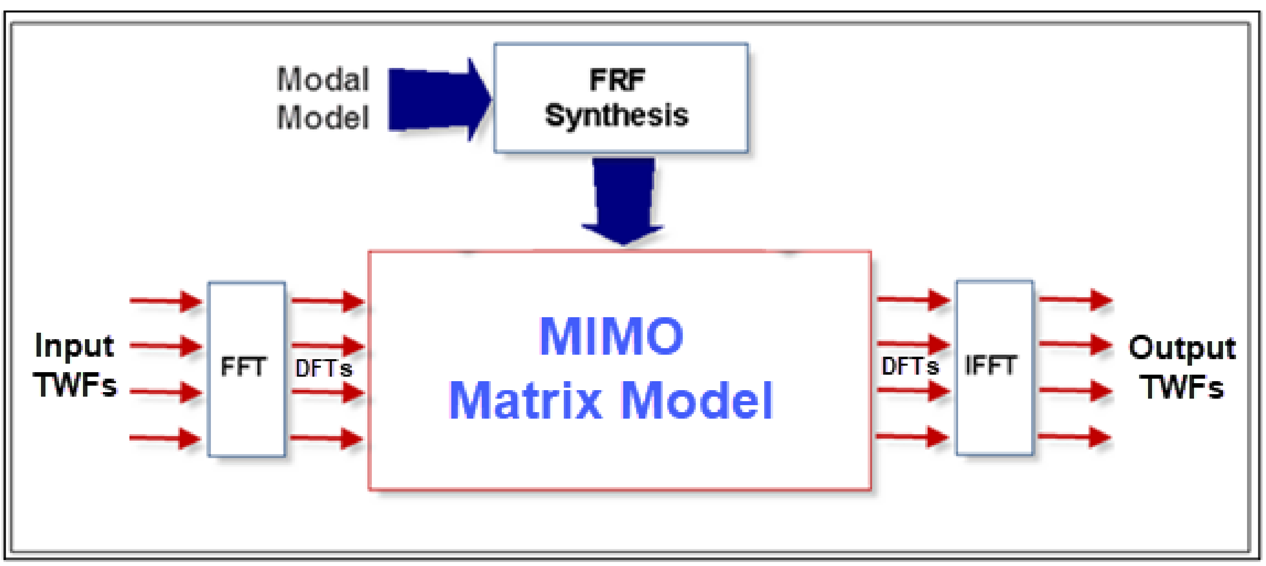

Figure 6 MIMO Calculation of Response TWFs from Internal Force TWFs & Mode Shapes

INTERNAL FORCE TWFs FROM CELLPHONE TWFs

Next, a modal model of the machine with mounting stiffnesses of **10,000 lbf/in** together with **response TWFs** extracted from a cellphone video of the actual operating machine were used to calculate the **internal force TWFs** necessary to cause the measured responses. This process is depicted in Figure **7A**.

Both the mounting stiffnesses and the internal forces of the machine are unknown. The mode shapes resulting from five different mounting stiffnesses would yield five different **internal force TWFs** for a single unbalance case. The **internal unbalance force TWFs** caused by mounting stiffness of **10,000 lbf/in** are displayed in Figure **7B**.

Figure 7B shows that the **unbalance forces** in the Y direction (vertical) are about ***3 times higher*** than the forces in the X-direction (horizontal) at points 1 & 2 **on the tops of the bearing blocks**.

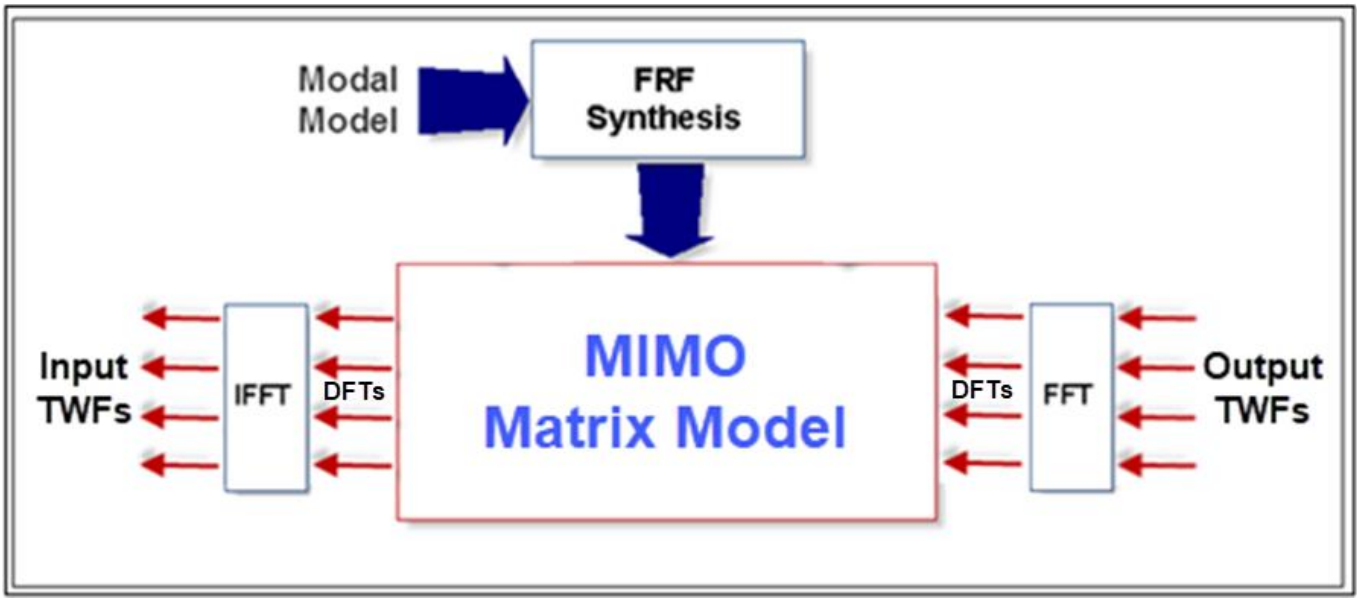

Figure 7A MIMO Calculation of Internal Force TWFs from Response TWFs & Mode Shapes

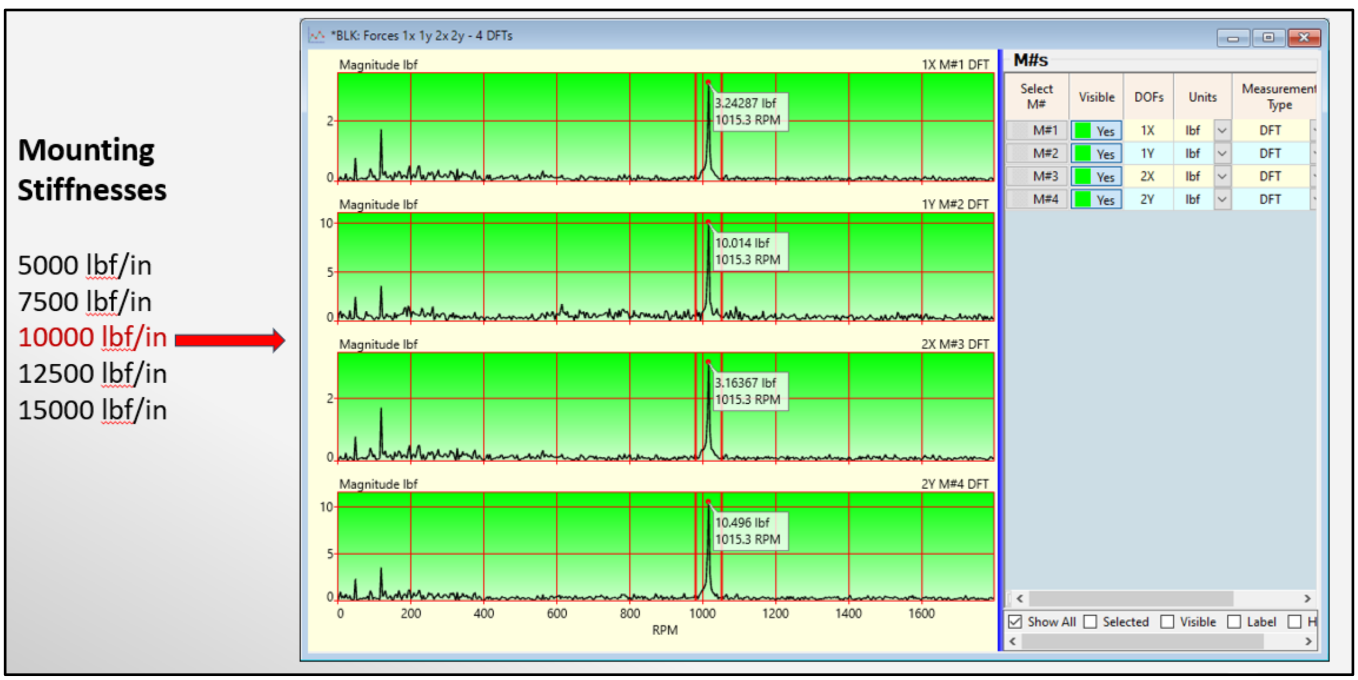

Figure 7B. Internal Force TWFs at Bearing Block Points 1 & 2

MACHINE RESPONSE TWFs FROM FRFS & INTERNAL FORCE TWFS

Using the modal model of the machine on springs with ***five different mounting stiffnesses*** and internal force **TWFs** with ***three different force levels***, machine response output **TWFs** were calculated using the **MIMO Matrix Model** depicted in Figure 6. Typical calculated **MIMO** response **DFTs** for points 1 & 2 on the tops of the bearing blocks is shown in Figure 8.

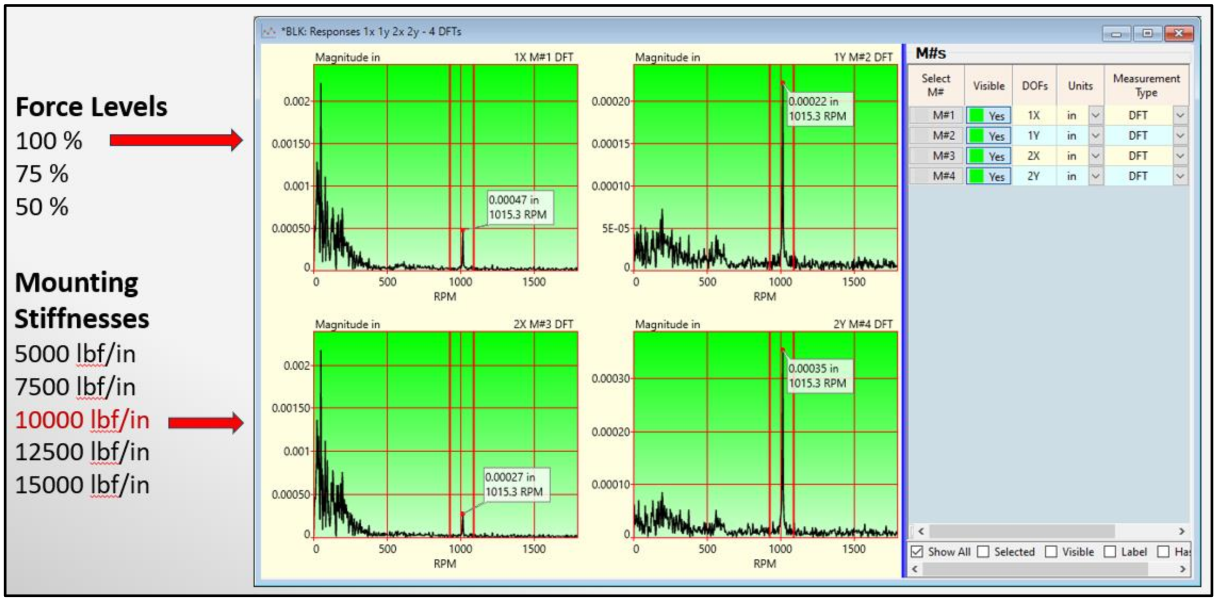

Figure 8. Response DFTs at Bearing Block Points 1 & 2

ARCHIVAL ODS DATABASE

The **MIMO Matrix Model** calculation depicted in Figure 6 was used in two calculation loops to calculate the response **TWFs** of the rotating machine using ***five machine mounting stiffnesses*** and ***three internal force levels***. The response **TWFs** for each stiffness and force level case were then processed to calculate **ODS-FRFs** for **points 1 & 2 at the top of the bearing blocks** for each case.

This calculation process is depicted in Figure 9.

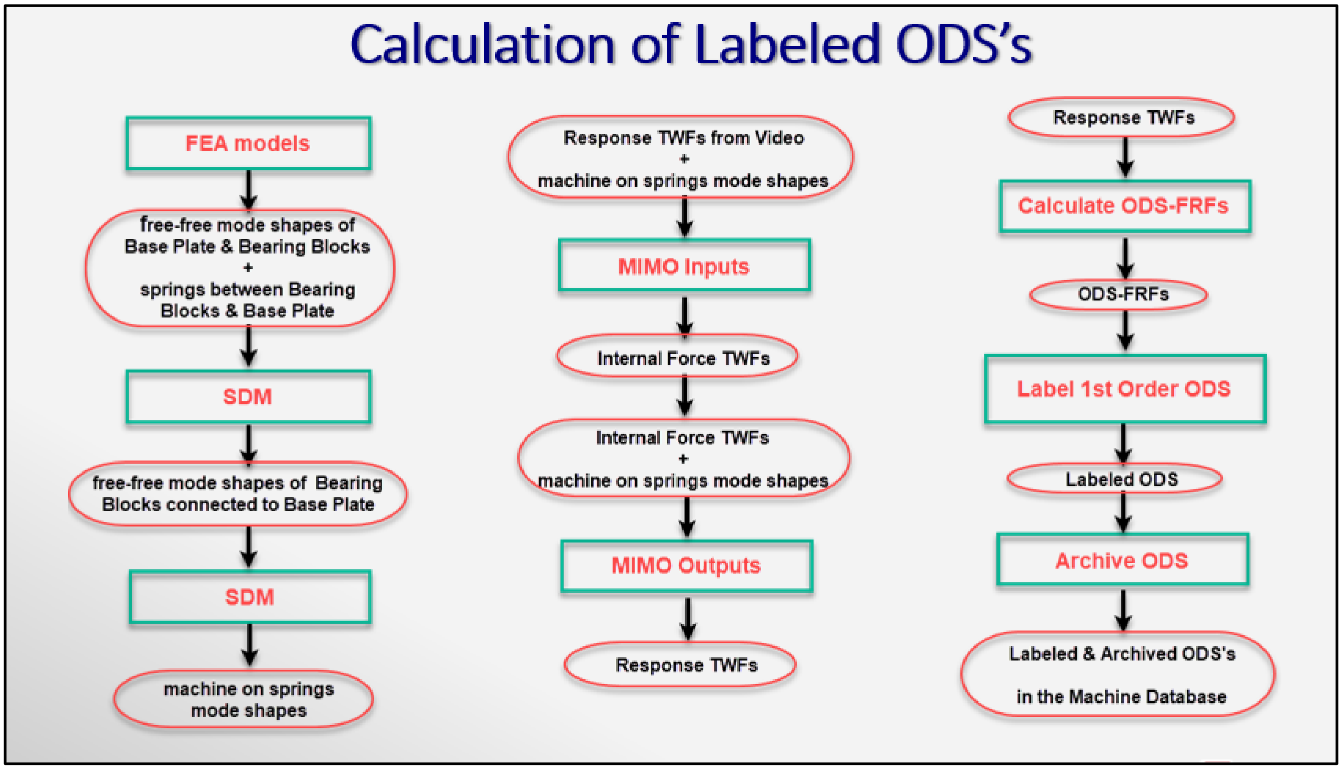

Figure 9. Calculation of ODS's for Mounting Stiffnesses & Force Levels

The cellphone video with ***four unbalance screws added to the outer rotor*** was chosen and labeled as the **Baseline**. Its **TWFs** were used together with a modal model for **mounting stiffnesses of 10000 lbf/in** to calculate internal force **TWFs** for the **Baseline**.

Then, **SDM** was used together with the free-free mode shapes of the machine to calculate new mode shapes of the machine for each of the ***five different mounting stiffnesses***. Each set of new mode shapes was used together with one of ***three different force levels*** to calculate response **TWFs** using the **MIMO Matrix Model** depicted in Figure 6.

The Baseline **ODS** together with the **first-order ODS's** extracted for the **ODS-FRFs** for ***all 15 combinations of five mounting stiffness & three internal force levels*** are shown in the Trend Plot Figure **10**. Each **ODS** has four **DOFs**, **1X, 1Y, 2X, 2Y** at points **1 & 2** at the **top of each bearing block**.

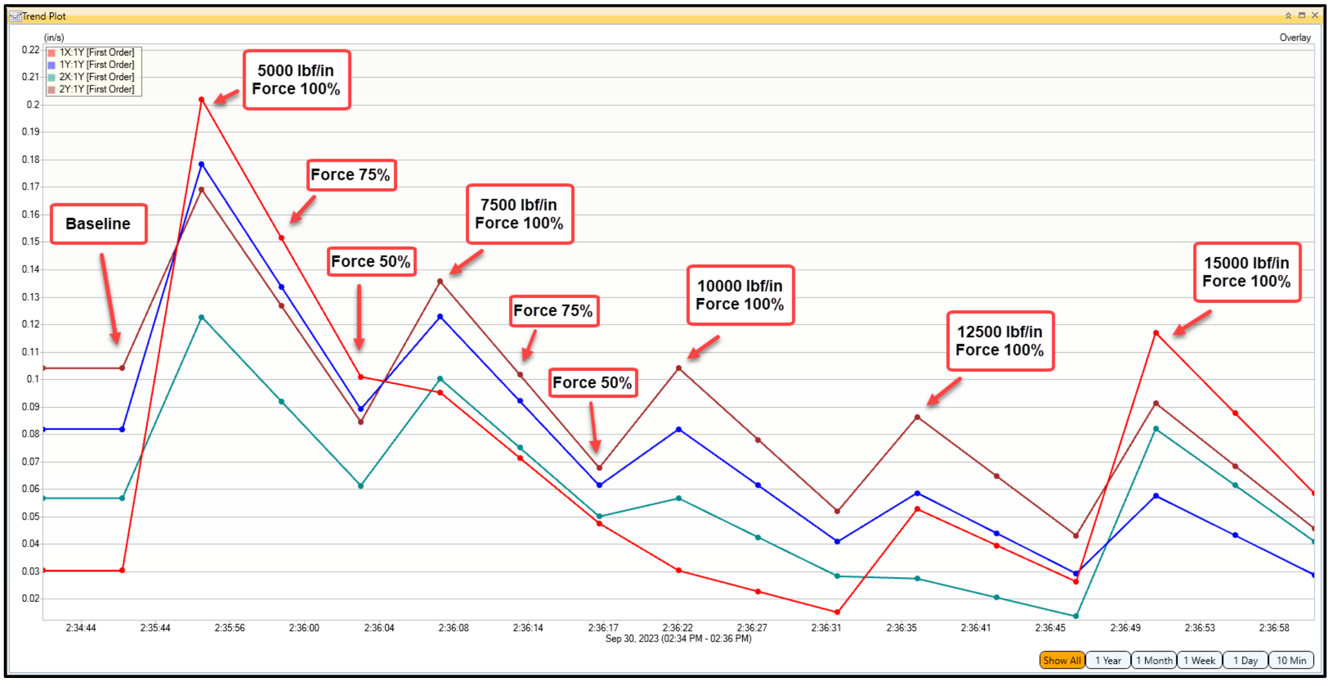

Figure 10. Velocity Trend Plot of Sixteen Labeled Stiffness & Force Level Cases

EVENT LOG

The Baseline **ODS** and the **ODS's** of fifteen mounting stiffness & internal force level cases are labeled as events in the archival database. The **Event Log** where the ODS's are labeled is shown in Figure **11**. Each of the sixteen cases is labeled in the Description column.

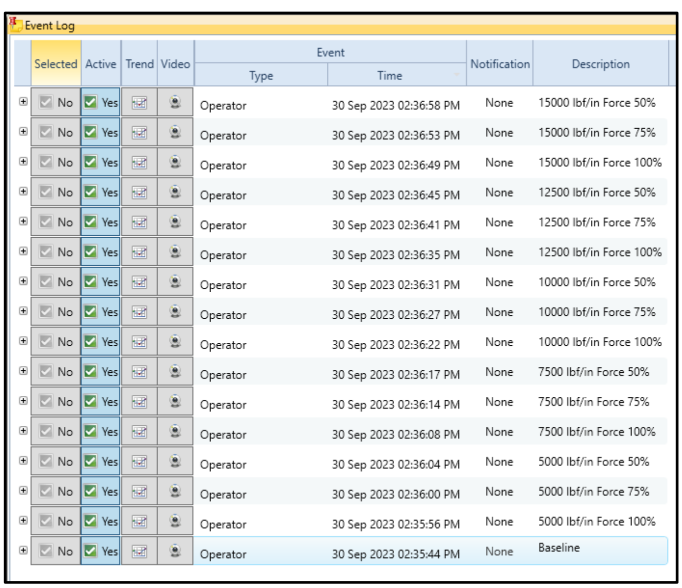

Selected	Active	Trend	Video	Event Type	Event Time	Notification	Description
No	Yes			Operator	30 Sep 2023 02:36:58 PM	None	15000 lbf/in Force 50%
No	Yes			Operator	30 Sep 2023 02:36:53 PM	None	15000 lbf/in Force 75%
No	Yes			Operator	30 Sep 2023 02:36:49 PM	None	15000 lbf/in Force 100%
No	Yes			Operator	30 Sep 2023 02:36:45 PM	None	12500 lbf/in Force 50%
No	Yes			Operator	30 Sep 2023 02:36:41 PM	None	12500 lbf/in Force 75%
No	Yes			Operator	30 Sep 2023 02:36:35 PM	None	12500 lbf/in Force 100%
No	Yes			Operator	30 Sep 2023 02:36:31 PM	None	10000 lbf/in Force 50%
No	Yes			Operator	30 Sep 2023 02:36:27 PM	None	10000 lbf/in Force 75%
No	Yes			Operator	30 Sep 2023 02:36:22 PM	None	10000 lbf/in Force 100%
No	Yes			Operator	30 Sep 2023 02:36:17 PM	None	7500 lbf/in Force 50%
No	Yes			Operator	30 Sep 2023 02:36:14 PM	None	7500 lbf/in Force 75%
No	Yes			Operator	30 Sep 2023 02:36:08 PM	None	7500 lbf/in Force 100%
No	Yes			Operator	30 Sep 2023 02:36:04 PM	None	5000 lbf/in Force 50%
No	Yes			Operator	30 Sep 2023 02:36:00 PM	None	5000 lbf/in Force 75%
No	Yes			Operator	30 Sep 2023 02:35:56 PM	None	5000 lbf/in Force 100%
No	Yes			Operator	30 Sep 2023 02:35:44 PM	None	Baseline

Figure 11 Event Log of Sixteen Mounting Stiffnesses & Force Levels

FaCTs™ - BASELINE CASE

When the **Baseline ODS** is archived into the database a second time, the **FaCTs** bar chart, (shown in Figure **12)**, clearly identifies it as the **ODS** for the Baseline case.

The **ODS's** for the **10000 lbf/in stiffness & 75% force leve**l case and the **12500 lbf/in & 100 force level** both ***closely correlate*** with the Baseline **ODS**.

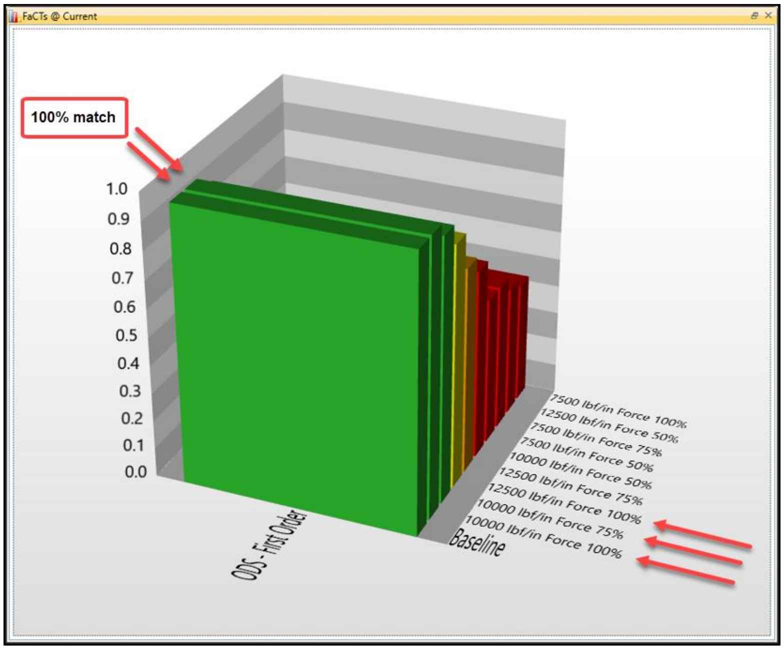

Figure 12. FaCTs™ for the Four Outboard Screws ODS

FaCTs™ - OUTBOARD ROTOR UNBALANCE CASES

Figures **13** through **15** show **FaCTs** correlations of **ODS's** for ***three cases of unbalance screws*** added to the **outboard rotor** of the rotating machine.

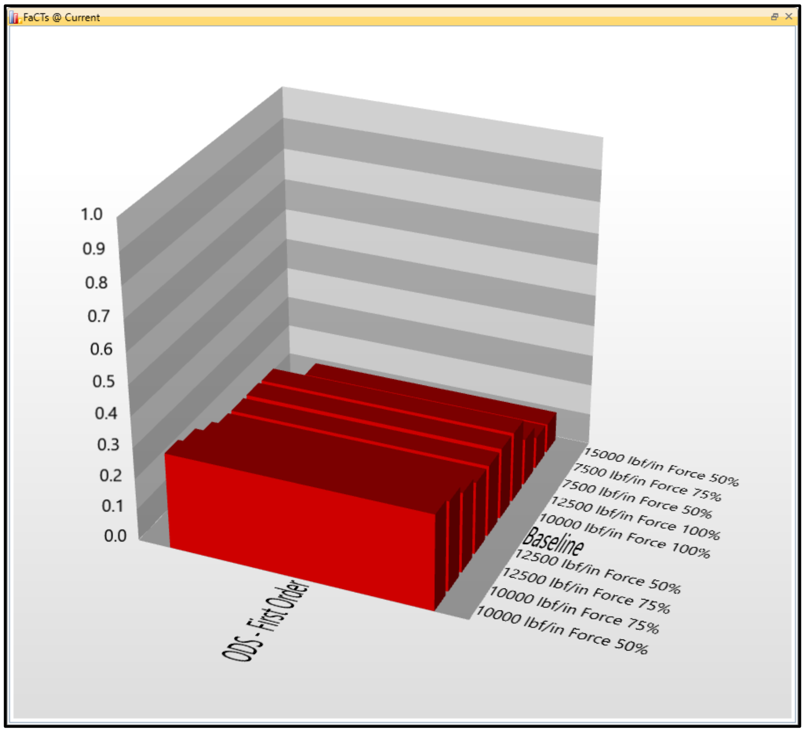

Figure 13. FaCTs™ for Three Outboard Screws

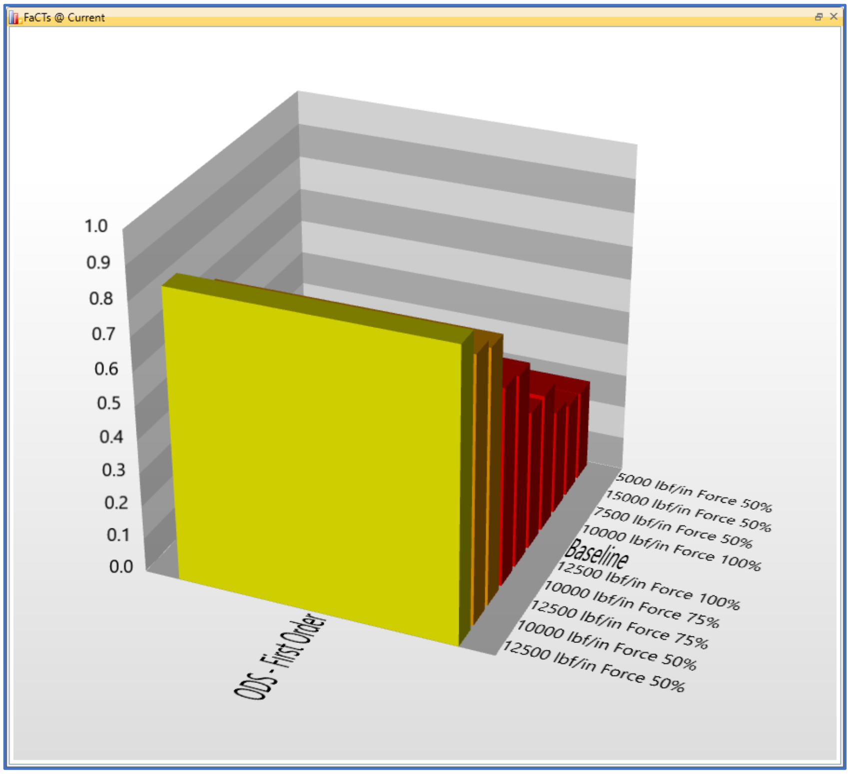

Figure 14. FaCTs™ for Two Outboard Screws

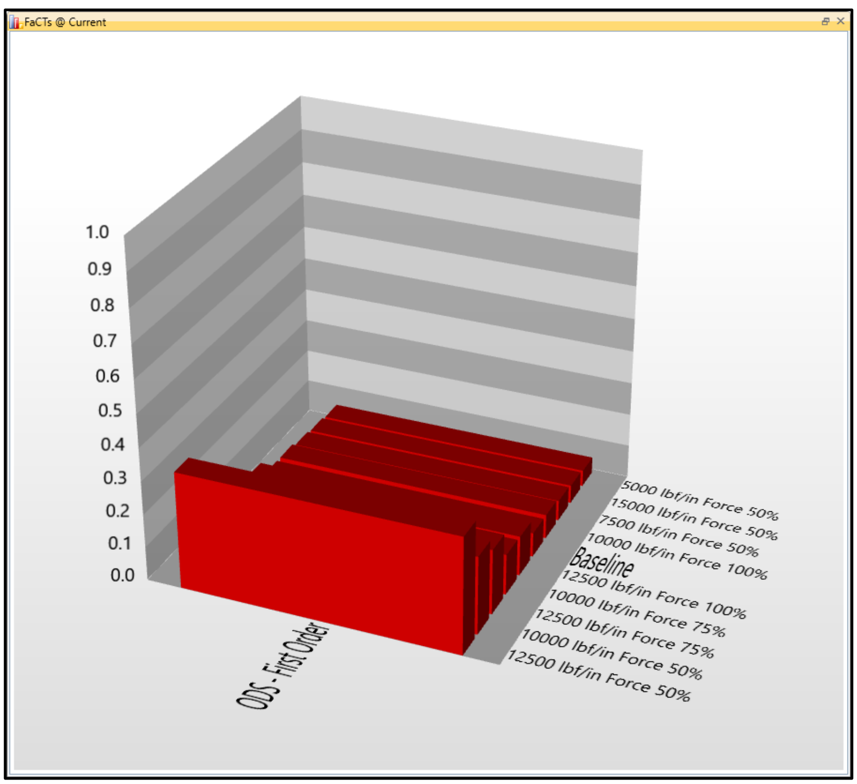

Figure 15. FaCTs™ for One Outboard Screw

All three **FaCTs** bar charts in Figures 13 to 15 indicate ***poor correlation*** between the three outboard unbalances and the baseline unbalance case. Clearly, the first-order ODS at the top of the bearing blocks is different for these cases.

FaCTs™ - INBOARD ROTOR UNBALANCE CASES

Figures **16** through **18** show **FaCTs** correlations of **ODS's** for **three cases of unbalance screws** added to the **inboard rotor** of the rotating machine.

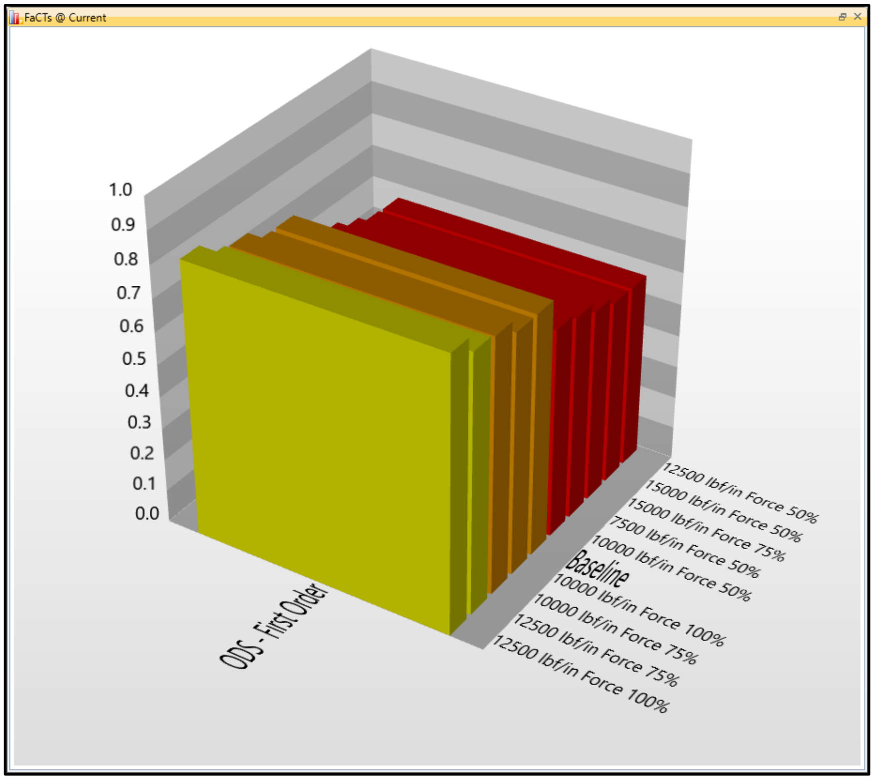

Figure 16. FaCTs™ for Four Inboard Screws

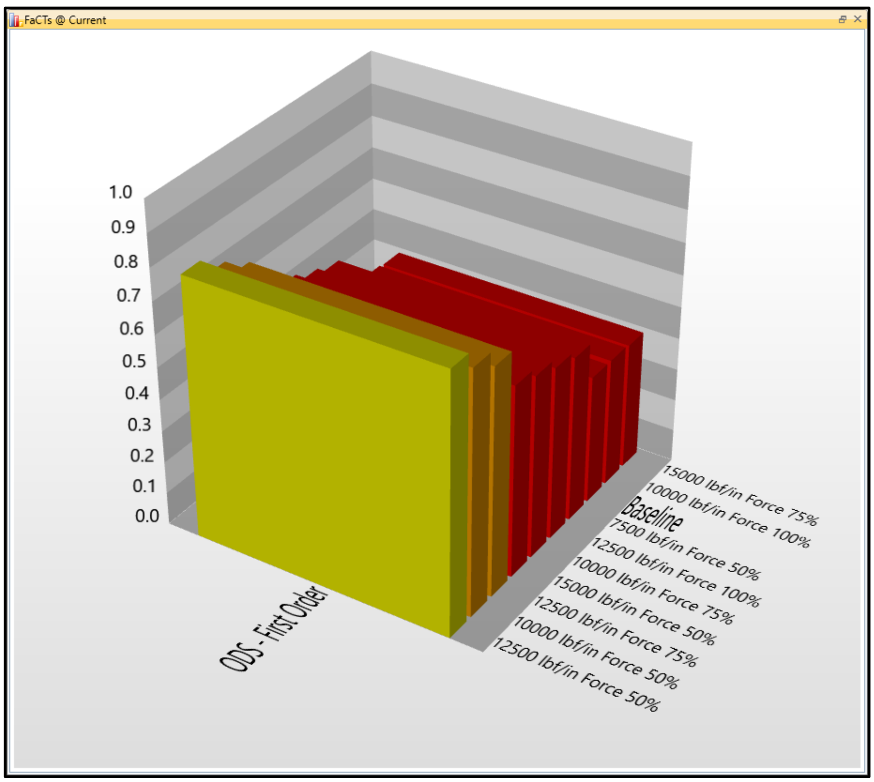

Figure 17. FaCTs™ for Two Inboard Screws

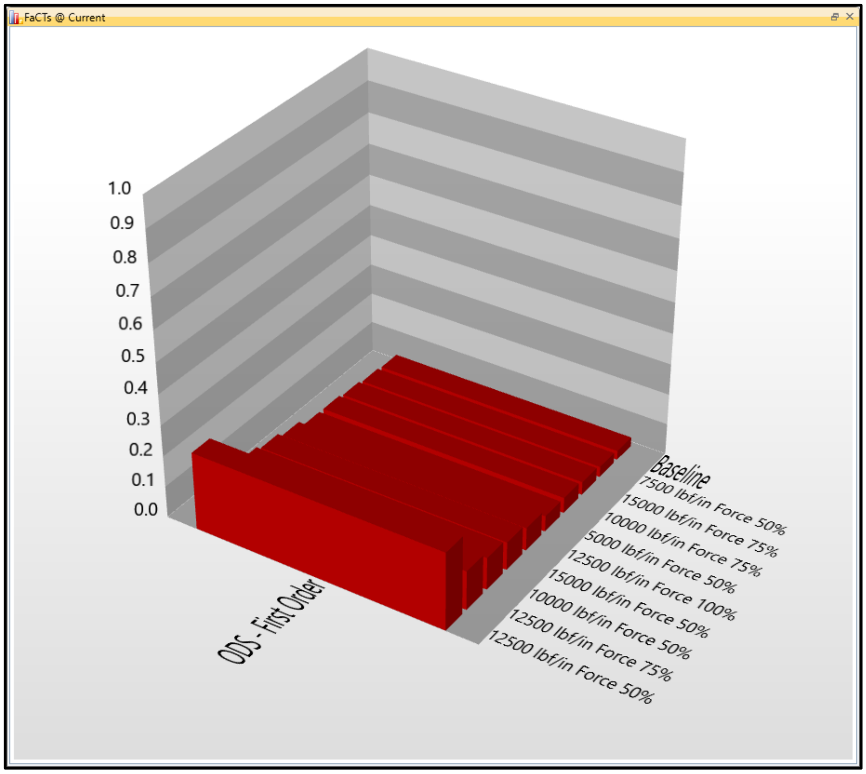

Figure 18. FaCTs™ for One Inboard Screw

Again, all three **FaCTs** bar charts in Figures 16 to 18 indicate ***poor correlation*** between the three inboard unbalances and the Baseline unbalance case. Again, the first-order **ODS** at the top of the bearing blocks is quite different for these three cases compared with the Baseline **ODS**.

CONCLUSIONS

In this paper, several signal processing methods were used to calculate the **first-order ODS** at the top of the bearing blocks of a rotating machine resulting from **five different mounting stiffnesses & three different internal force levels** of the machine. The free-free mode shapes of the **base plate & bearing blocks** of the machine were used together with the **SDM** method to calculate the new mode shapes of the machine mounted on springs with different stiffnesses between the corners of its base plate and ***"fixed***" ground points on a tabletop. Five different stiffness values were used for the four axial springs connected between the plate corners and the fixed tabletop.

Using the modal model for **10000 lbf/in** of a mounting stiffness, **MIMO Matrix** processing was used to calculate the internal force **TWFs** necessary to yield the response **TWFs** extracted from a cellphone video of the machine. The Baseline video was recorded with **four unbalance screws** attached to the **outboard rotor** and the machine running at **about 1000 RPM**. The response **ODS** for this case was labeled as the **Baseline ODS**.

Response TWFs were then calculated for 15 different cases, using all combinations of **five different mounting stiffnesses & three different internal force levels**. **ODS-FRFs** were then calculated from each response **TWF**, and the **first-order ODS** at **1000 RPM** was labeled and saved in an archival database.

All the digital signal processing and **ODS** labeling was done automatically by executing a **command script** in MEscope.

Finally, a unique database search method called **FaCTs™** was used to correlate the **ODS's** derived from cellphone videos of **eight different unbalance** cases of the rotating machine with the **16 labeled ODS's** in an archival database.

The **FaCTs** bar charts clearly identified the **Baseline ODS** of the machine with four unbalance screws on the outboard rotor and **10000 lbs/in** of mounting stiffness at the corners of the rotating machine. The **FaCTs** bar charts also showed that most of the other unbalance screw cases ***were not closely correlated*** with any of the labeled **ODS's** in the database.

The methods used in this exercise showed that mode shapes and **MIMO Matrix Modeling** can be used to calculate and label **ODS's**, and then use the labeled and archived **ODS**'s to characterize machine faults. In this paper, a common machine problem called ***"soft foot"*** was addressed.

However, just like in the training of a neural network, much more **labeled ODS** data for a machine must be added to the archival database to identify and quantify a mechanical fault such as soft foot more accurately.

Nevertheless, the precise identification of the Baseline case using **FaCTs™** from the **first-order ODS** for only **2 DOFs** at the top of each bearing block is confirming evidence that using **SDM** with free-free mode shapes, **MIMO Matrix Modeling**, and **ODS-FRF** calculations are all **linear repeatable calculations**. This exercise demonstrates that all these calculations can be used reliably to characterize the **linear dynamic behavior** of real-world rotating machines and mechanical structures.

REFERENCES

[1] - Farnebäck G. (2003) Two-Frame Motion Estimation Based on Polynomial Expansion. In: Bigun J., Gustavsson T. (eds) Image Analysis. SCIA 2003. Lecture Notes in Computer Science, vol 2749. Springer, Berlin, Heidelberg

[2] - https://nanonets.com/blog/optical-flow/

[3] - B. Schwarz, S. Richardson, J. Tyler, R. Spears, M. Richardson, "Post-Processing **ODS** Data from a Vibration Video" IMAC XXXVIII Houston, TX, February 10-13, 2020.

[4] - M.H. Richardson, "Is It a Mode Shape or an Operating Deflection Shape?" Sound and Vibration magazine, March 1997.

[5] - B. Schwarz, M.H. Richardson, "Measurements Required for Displaying Operating Deflection Shapes" Proceedings of IMAC XXII, January 26, 2004

[6] - B. Schwarz, M.H. Richardson, "Introduction to Operating Deflection Shapes" CSI Reliability Week, Orlando, FL, October 1999

[8] - D. Ambre, B. Schwarz, S. Richardson, M. Richardson, "Using Cellphone Videos to Diagnose Machinery Faults" IMAC XLI, February 13-16, 2023, Austin, TX.

[9] - MEscope™ is a trademark of Vibrant Technology, Inc. www.vibetech.com

[10] - B. Schwarz, S. Richardson, P. McHargue, M. Richardson "Using Cellphone Videos to Diagnose Unbalance in Machinery" IMAC XLII, January 29 - February 1, 2024, Orlando, TX

[11] - S. Richardson, J. Tyler, P. McHargue, M. Richardson "A New Measure of Shape Difference" IMAC XXXII February 3.6, 2014

[12] – "B. Schwarz, P. McHargue, M. Richardson "Using SDM to Train Neural Networks for Solving Modal Sensitivity Problems" 14th IMAC Conference, Dearborn, MI, February 1996